Supplementary figure 1

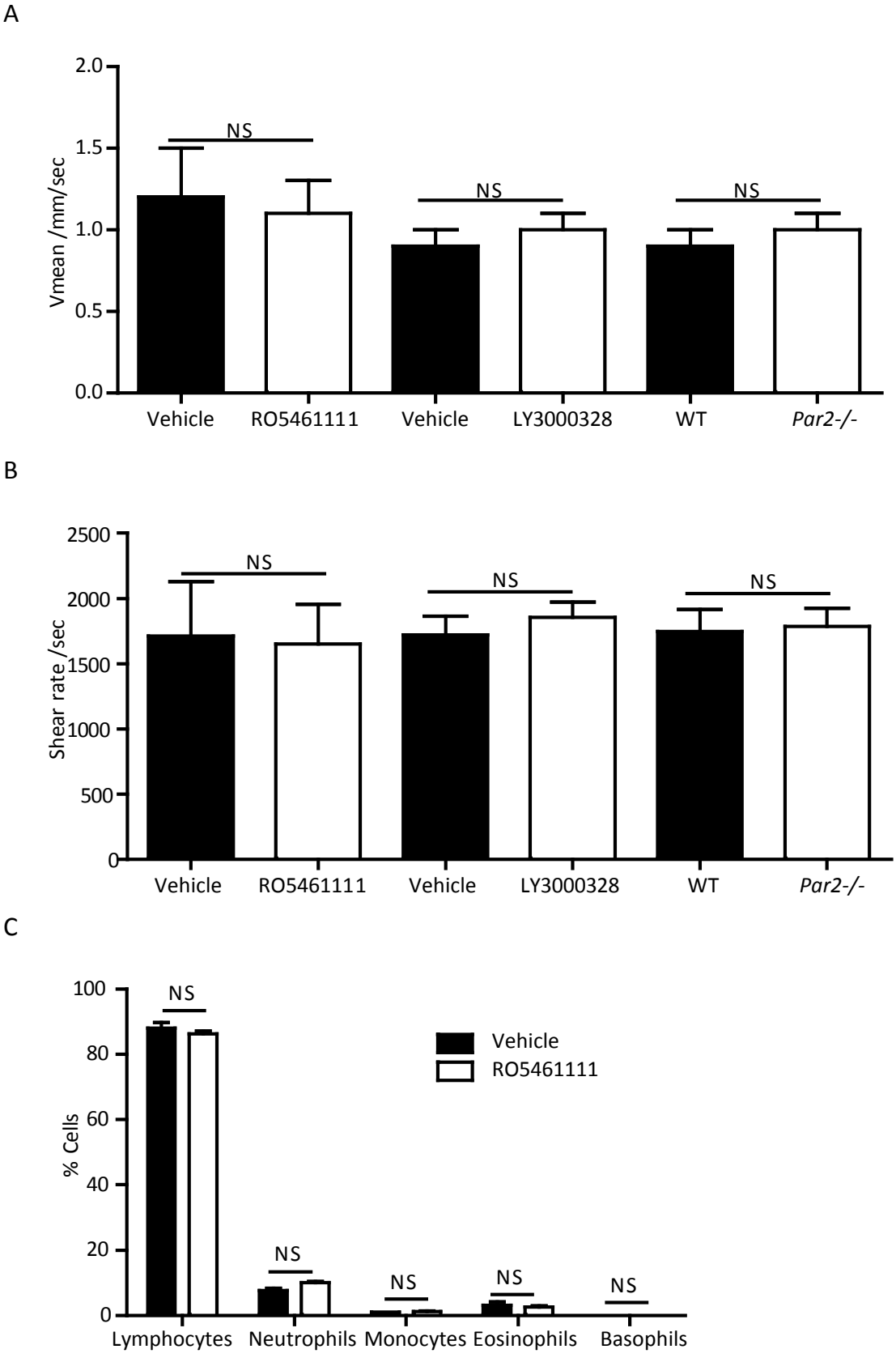

Figure S1. Hemodynamic parameters and white blood counts in peripheral blood upon Cat-S blockade in C57BL/6 mice. In vitro microscopy of postcapillary venues of cremaster muscles requires stable hemodynamic parameters. Mean velocity (Vmax) and shear rate are shown in A and B, respectively. C: Peripheral white blood count after administration of the Cat-S inhibitor was unaffected. D: Also blood leukocyte flow cytometry after 6 weeks of RO5461111 feeding showed no significant (NS) effects on leukocyte subpopulations. Data are means ± SEM of at least 5 mice in each group.

Supplementary figure 2

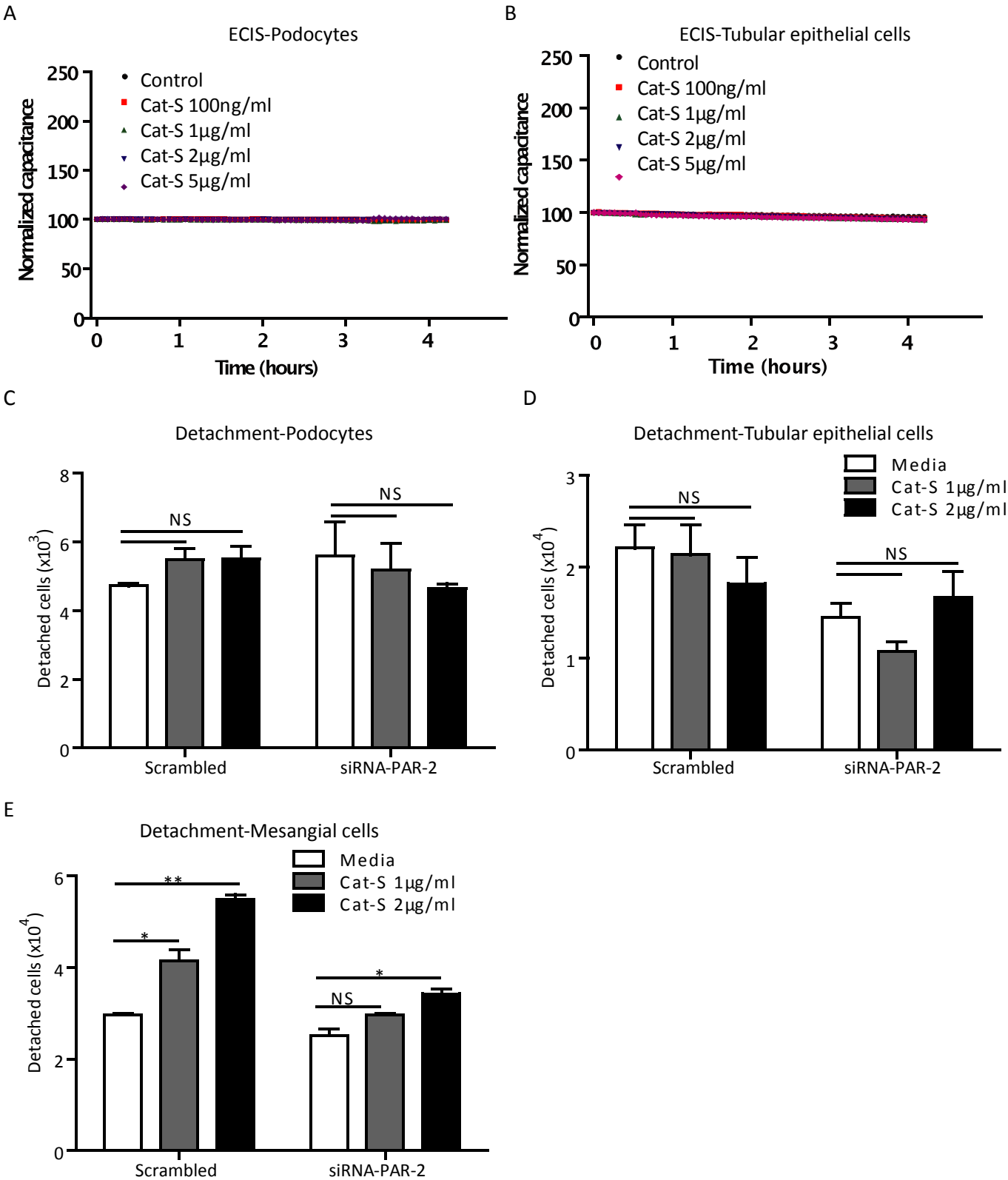

Figure S2. Cathepsin S does not affect podocytes or tubular epithelial cells but induces endothelial cell death via PAR2. In vitro Electric Cell Substrate Impedance Sensing (ECIS) studies with murine podocytes (A) or tubular epithelial cells (TECs, B). Cell monolayers were exposed to increasing doses of Cat-S and cell capacitance was determined at 40 kHz over a period of 4 hours. Note that none of the doses affect cell capacitance. Graphs are readings of single experiments representative of at least 3 experiments for each condition. Pdocytes (C), tubular epithelial cells (D), and mesangial cells (E) were transfected with PAR2 siRNA or scrambled siRNA stimulation with different concentrations of Cat-S (1 and 2µg/ml) for 20 hours and detachment of cells was analyzed.. Data are means ± SEM of three independent experiments. * $p<0.05$, *$p<0.01$ versus scrambled RNA sequence control, NS = not significant.

Supplementary figure 3

A

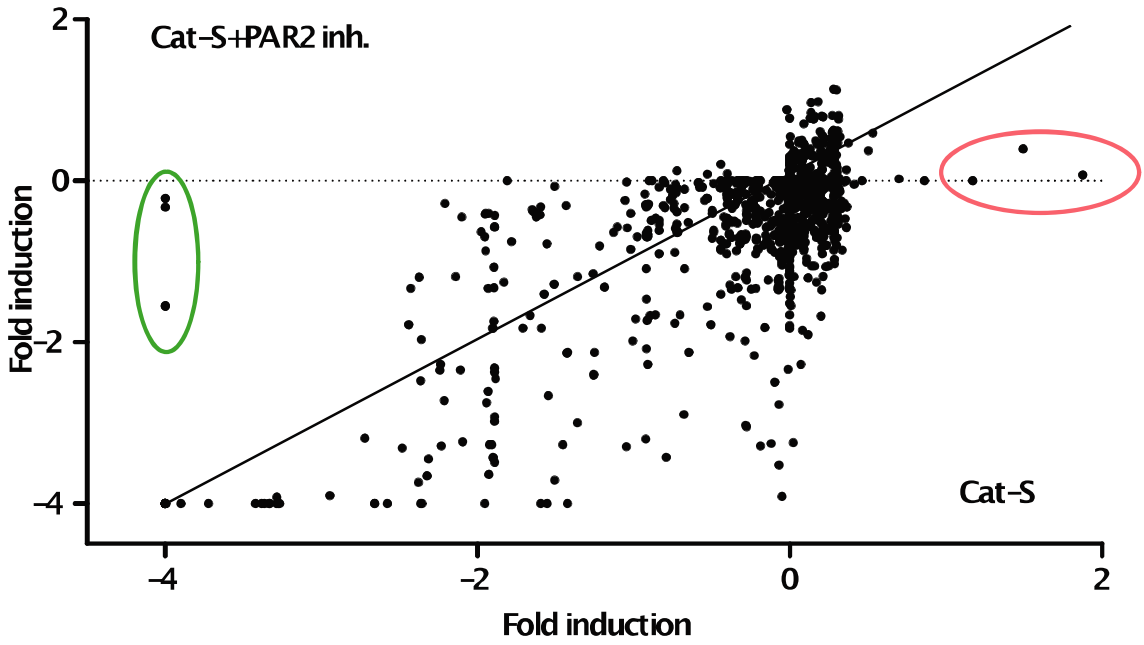

B

S.No.	Reactome or Nature ID	Cat-S	Cat-S + PAR2 inh.
1	MITOTIC_ANAPHASE_REACTOME	-4,0	-1,6
2	MITOTIC_METAPHASE_AND_ANAPHASE_REACTOME	-4,0	-1,6
3	MITOTIC_PROMETAPHASE_REACTOME	-4,0	-0,2
4	RESOLUTION_OF_SISTER_CHROMATID_COHESION_REACTOME	-4,0	-0,3
5	SEPARATION_OF_SISTER_CHROMATIDS_REACTOME	-4,0	-1,6
1	AMINO_ACID_AND_OLIGOPEPTIDE_SLC_TRANSPORTERS_REACTOME	1,5	0,4
2	AMINO_ACID_TRANSPORT_ACROSS_THE_PLASMA_MEMBRANE_REACTOME	1,9	0,1
3	PRESENILIN_ACTION_IN_NOTCH_AND_WNT_SIGNALING_NCI_NATURE	1,2	0,0

Figure S3. Gene array studies with glomerular endothelial cells. Affymetrix gene array analysis performed on glomerular endothelial cells exposed to Cat-S or Cat-S plus PAR2 inhibitor. A: Signaling networks from REACTOME are shown, where each point in the diagram corresponds to one network. Each network is characterized by a score, which is the negative logarithm (to the base of 10) of the FDR-corrected q value for enrichment. Positive scores indicate up-regulation of networks, negative scores the opposite. The three networks circled in green are induced with Cat-S but entirely blocked in the presence of PAR2 inhibitor. The five networks circled in red that are strongly down-regulated by Cat-S alone, but again reversed by presence of PAR2 inhibitor. B: The table lists up-regulated (in green) and down-regulated (in red) indicated in A.

Supplementary figure 4

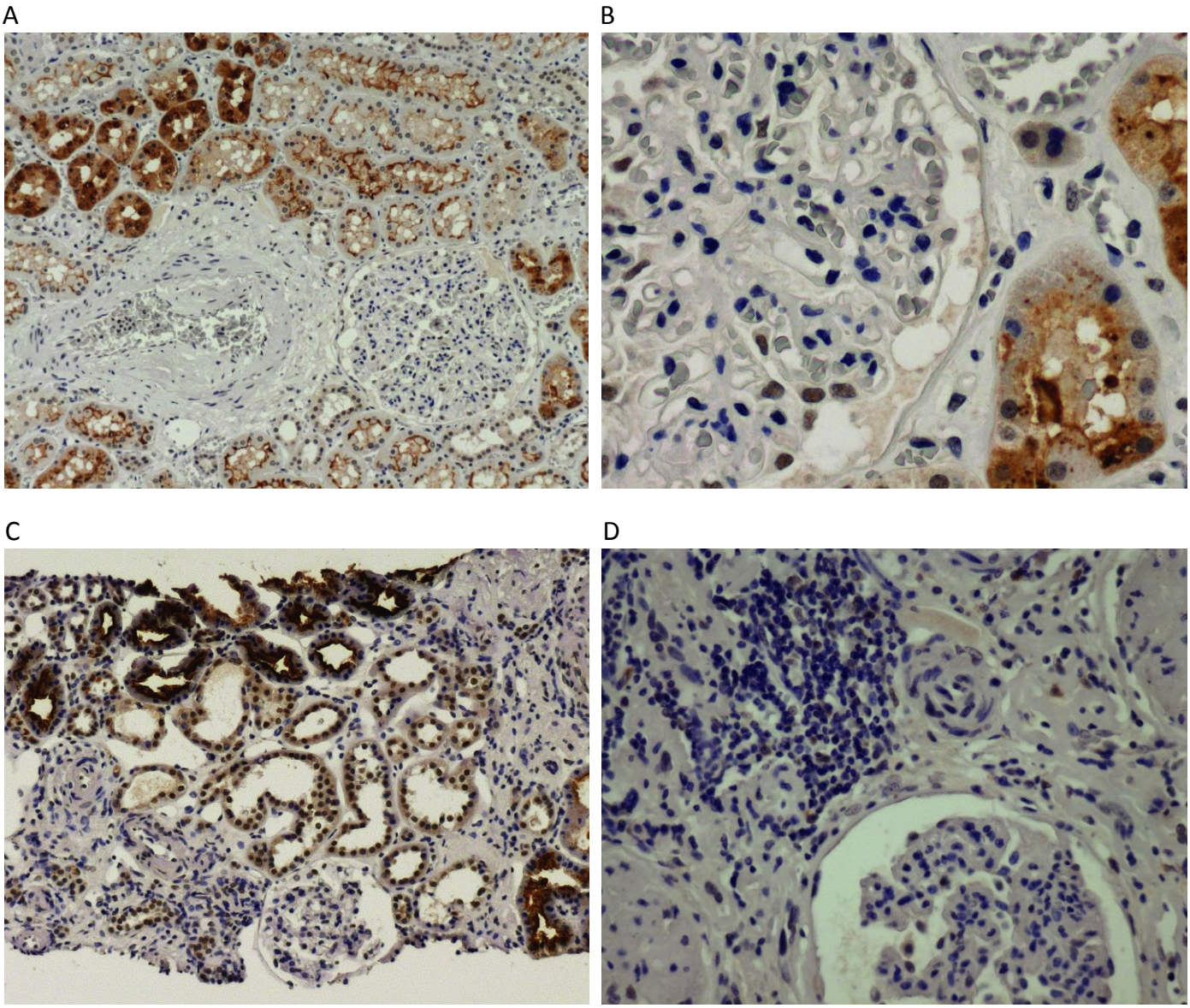

Figure S4. Cystatin C immunostaining of human diabetic nephropathy. In early diabetic nephropathy the positive signal is intense in proximal tubules, less in distal tubules and absent in glomeruli or interstitial cells (A and B). In advanced diabetic nephropathy with tubular atrophy and interstitial fibrosis, cystatin C positivity is not evident in interstitial cell infiltrates but single glomerular epithelial cells display some nuclear positivity. Original magnification 100x, 200x, 400x.

Supplementary figure 5

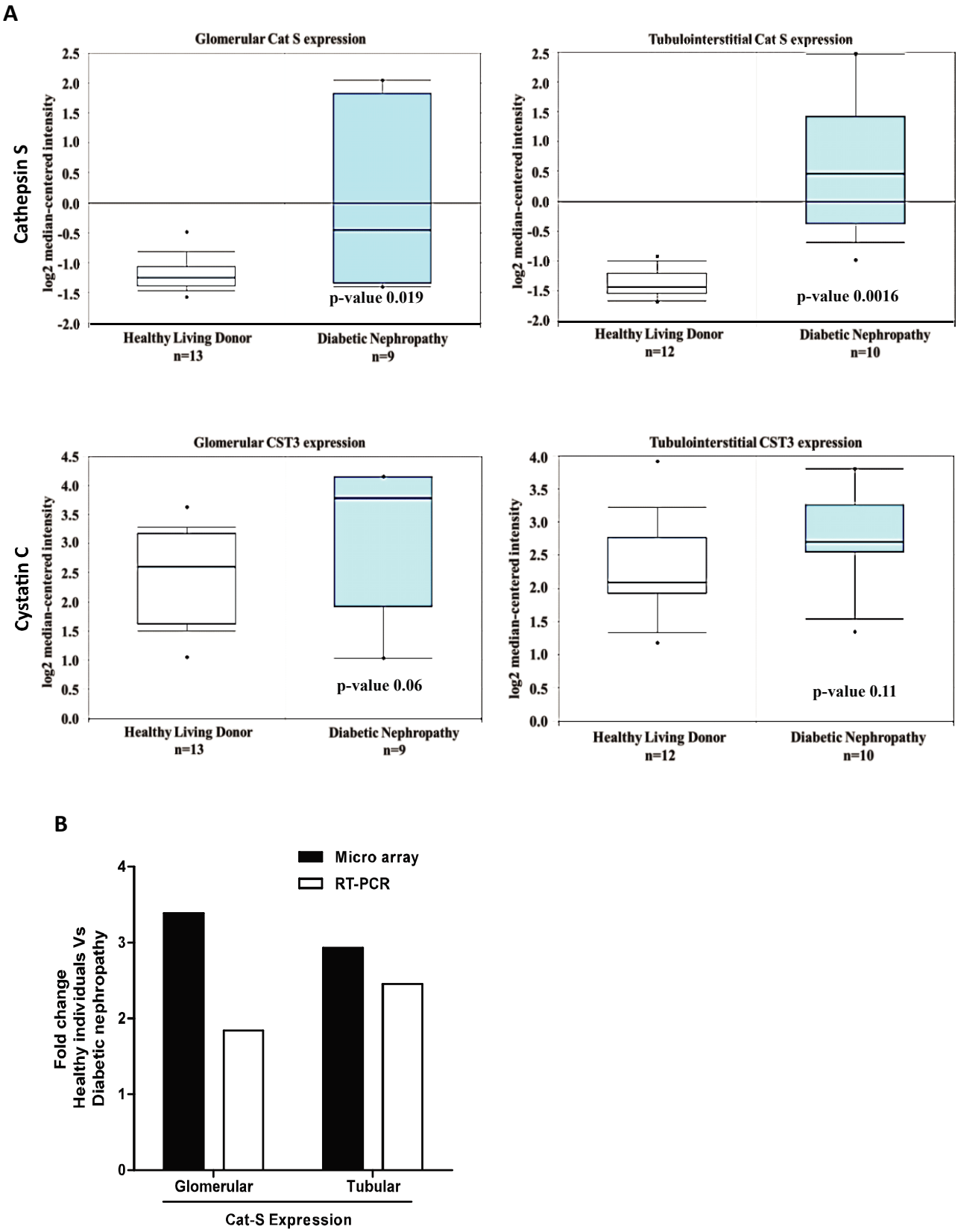

Figure S5. Cathepsin S and cystastin C mRNA expression levels in human diabetic nephropathy. A: Gene expression data were obtained from microarrays of microdissected glomeruli and tubulointerstitial preparations from kidney biopsies of patients with diabetic nephropathy and living donors as controls. Nephromine (Compendia Bioscience, Ann Arbor, MI, USA, supported by the O'Brien Kidney Core Center at the University of Michigan) was used for analysis and visualization. Cat-S mRNA levels (CTSS gene) were significantly higher in diabetic nephropathy compared to controls, while the mRNA levels of cystatin C (CST3 gene) were not significantly different among the groups. Data are box blots of the log2 median-centred intensity ± SEM of the indicated sample numbers. Black dots indicate minimal and maximal values. B: Indicates the fold changes of the mRNA expression in diabetic patients versus controls as identified by microarray (black bars) as well as their validation by real-time PCR (white bars).

Supplementary figure 6

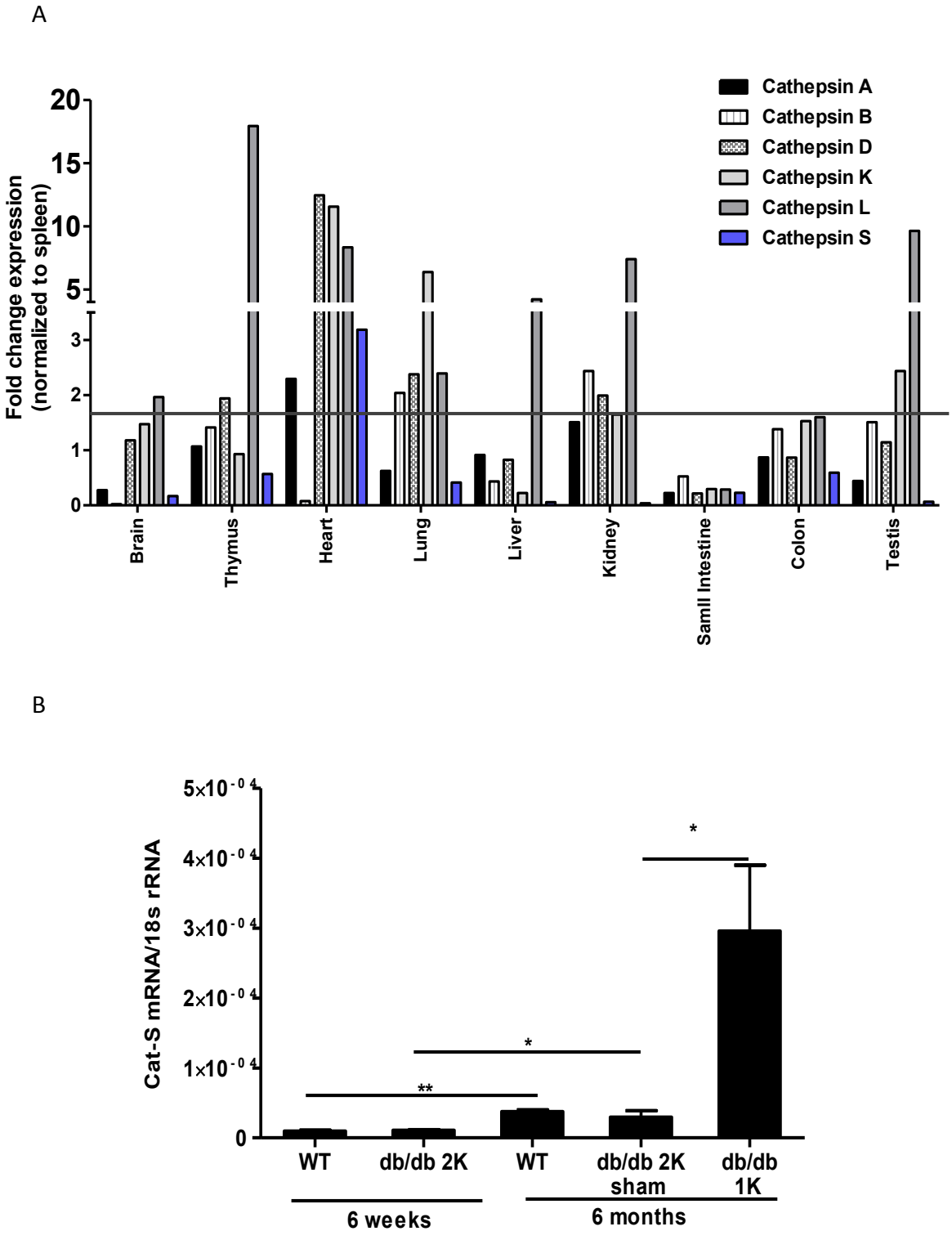

Figure S6. Expression of cathepsin mRNA in organs of C57BL/6 and db/db mice. A: Solid organs were harvested from 6 weeks old male C57BL/6 mice and mRNA expression was quantified for various cathepsins as indicated. Data are expressed as relative expression of each cathepsin to its respective mRNA levels in spleen. B: Renal Cat-S mRNA expression was quantified in 6 week and 6 month old male C57BL/6 or db/db mice. Mice (n=5 or more in each group) that underwent sham surgery with 2 kidneys (2K) or uninephrectomy (1K) were compared. * $p<0.05$, ** $p<0.01$.

Supplementary figure 7

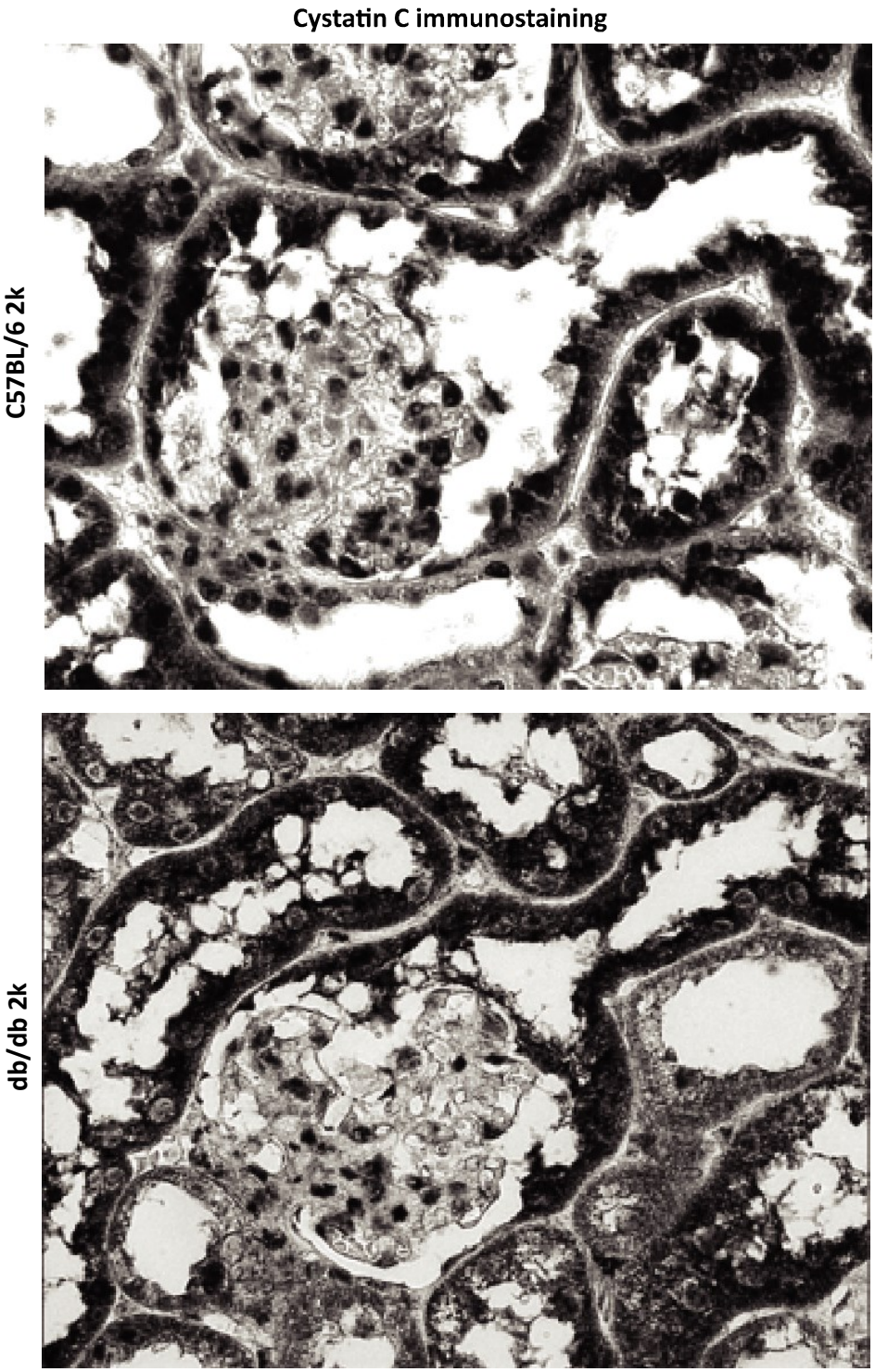

Figure S7. Renal cystatin C immunostaining in diabetic and non-diabetic mice. Cystatin C positivity showed an identical intensity and distribution pattern in non-diabetic and diabetic mice at 6 months of age. Representative images are shown at a magnification of 400x.

Supplementary figure 8

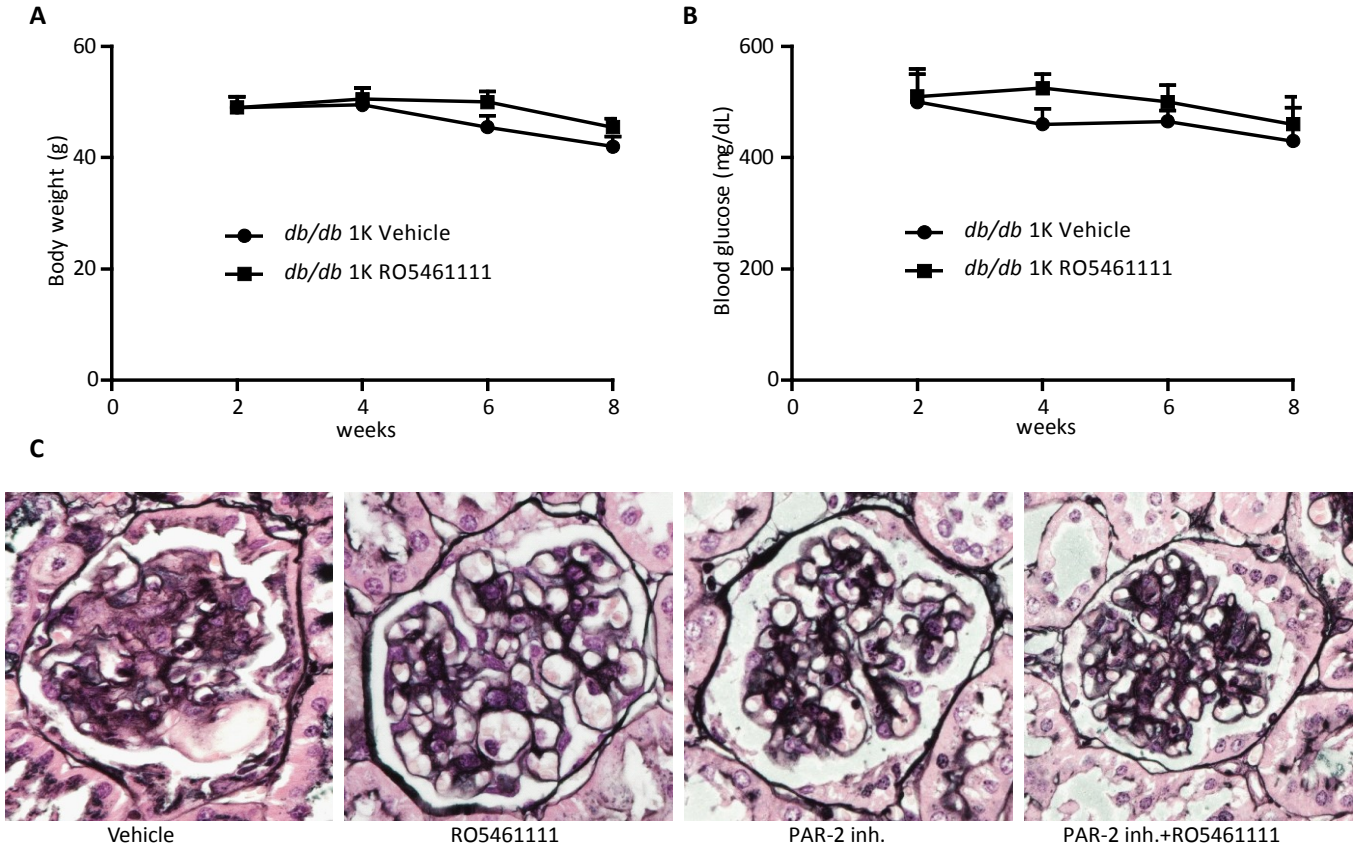

Figure S8. Cathepsin inhibition and body weight, blood glucose levels and extracellular matrix deposition in db/db mice. 8 weeks of RO5461111 feeding did not affect body weight (A) and blood glucose levels (B) in uninephrectomized db/db mice. Data are means ± SEM from 8-10 mice in each group. C: Silver staining showed an increased glomerular positivity in uninephrectomized (1K) kidneys of db/db mice, while Cat-S inhibition with RO5461111 and PAR-2 inhibition and combination reduced this aspect. Representative images are shown at a magnification of 400x.

Supplementary figure 9

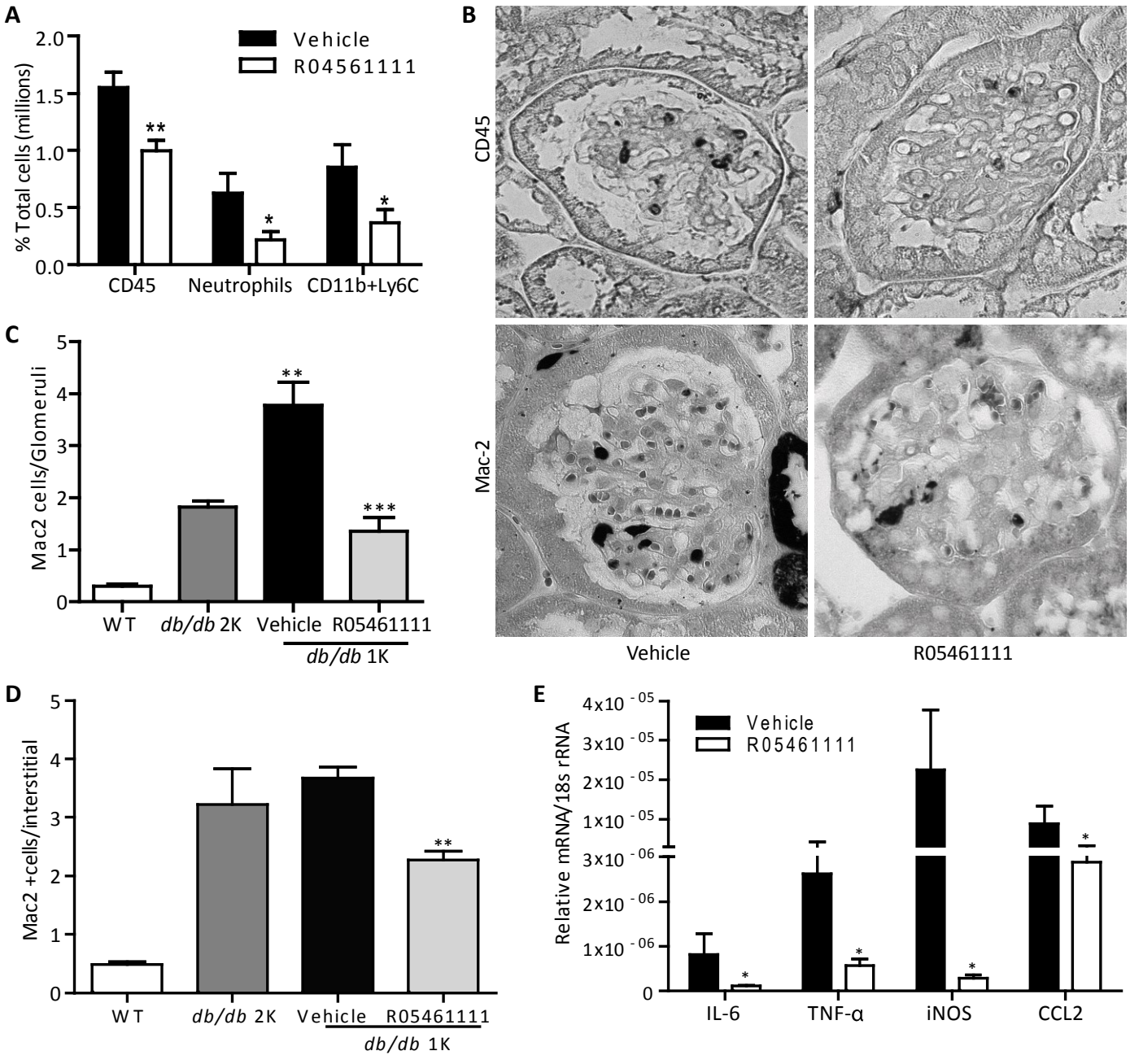

Figure S9. Cathepsin inhibition reduces renal leukocyte infiltration in db/db mice. A: Flow cytometry of kidney cell suspension of 1K db/db mice was used to quantify intrarenal CD45+ leukocytes, Ly6G+ neutrophils, and CD11b/Ly6C+ mononuclear phagocytes. B-D: Renal sections from both vehicle- and RO5461111-treated 1K db/db mice were stained for CD45 and Mac2 (original magnification x400). Data are shown as mean numbers of positive cells in 15 glomeruli or high power fields ± SEM. E: mRNA isolates from kidneys of 1K db/db mice underwent quantitative real-time PCR for a number of genes as indicated. Data are expressed as means of the ratio of the specific mRNA versus that of 18S rRNA ± SEM. * $p<0.05$, ** $p<0.01$, *** $p<0.001$ versus vehicle group.

Supplementary table 1

Gene			Sequence
Cathepsin-A	Forward	:	AGAGCGGTCAGGCCAAGACG
	Reverse	:	CGCGGTTCCGGGCATCTCTG
Cathepsin-B	Forward	:	CTGCGCGGGTACTTAGGAGT
	Reverse	:	CAGGCAAGAAAGAAGGATCAAG
Cathepsin-D	Forward	:	TTCGTCCTCCTTCGCGATT
	Reverse	:	TCCGTCATAGTCCGACGGATA
Cathepsin-K	Forward	:	GCCAGGATGAAAGTTGTATG
	Reverse	:	CAGGCGTTGTTCTTATTCC
Cathepsin-L	Forward	:	GTGGACTGTTCTCACGCTCA
	Reverse	:	TATCCACGAACCCTGTGTCA
Cathepsin-S	Forward	:	AAGCGGTGTCTATGACGACCC
	Reverse	:	GAGTCCCATAGCCAACCACAAG
IL6	Forward	:	TGATGCACTTGCAGAAAACA
	Reverse	:	ACCAGAGGAAATTTTCAATAGGC
TNF-α	Forward	:	AGGGTCTGGGCCATAGAACT
	Reverse	:	CCACCACGCTCTTCTGTCTAC
iNOS	Forward	:	TTCTGTGCTGTCCCAGTGAG
	Reverse	:	TGAAGAAAACCCCTTGTGCT
Ccl2	Forward	:	CCTGCTGTTCACAGTTGCC
	Reverse	:	ATTGGGATCATCTTGCTGGT
Nphs2 (Podocin)	Forward	:	TGACGTTCCCTTTTTCCATC
	Reverse	:	CAGGAAGCAGATGTCCCAGT
Nphs1 (Nephrin)	Forward	:	TTAGCAGACACGGACACAGG
	Reverse	:	CTCTTTCTACCGCCTCAACG
18s	Forward	:	GCAATTATTCCCCATGAACG
	Reverse	:	AGGGCCTCACTAAACCATCC

Table S1. List of primers used in the study